




REVIEW ARTICLE

Elucidating the microscopic and computational techniques to study the structure and pathology of SARS-CoVs

Sindhoora Kaniyala Melanthota¹  | Soumyabrata Banik¹  | Ishita Chakraborty¹ | Sparsha Pallen² | Dharshini Gopal² | Shweta Chakrabarti² | Nirmal Mazumder¹ 

¹Department of Biophysics, Manipal School of Life Sciences, Manipal Academy of Higher Education, Manipal, Karnataka, 576104, India

²Department of Bioinformatics, Manipal School of Life Sciences, Manipal Academy of Higher Education, Manipal, Karnataka, 576104, India

Correspondence

Nirmal Mazumder, Department of Biophysics, Manipal School of Life Sciences, Manipal Academy of Higher Education, Manipal, Karnataka, 576104, India.
Email: nirmaluva@gmail.com

Funding information

Science and Engineering Research Board, Grant/Award Number: ECR/2016/001944

Abstract

Severe Acute Respiratory Syndrome Coronaviruses (SARS-CoVs), causative of major outbreaks in the past two decades, has claimed many lives all over the world. The virus effectively spreads through saliva aerosols or nasal discharge from an infected person. Currently, no specific vaccines or treatments exist for coronavirus; however, several attempts are being made to develop possible treatments. Hence, it is important to study the viral structure and life cycle to understand its functionality, activity, and infectious nature. Further, such studies can aid in the development of vaccinations against this virus. Microscopy plays an important role in examining the structure and topology of the virus as well as pathogenesis in infected host cells. This review deals with different microscopy techniques including electron microscopy, atomic force microscopy, fluorescence microscopy as well as computational methods to elucidate various prospects of this life-threatening virus.

Highlights

- Structural analysis of SARS-CoVs aids in understanding its nature, activity, and pathophysiology
- Revealing the surface morphology of SARS-CoVs using scanning electron microscope and atomic force microscopy
- Computational methods help to understand the structure of SARS-CoVs and their interactions with various inhibitors

KEYWORDS

atomic force microscopy, computational biology, coronavirus, electron microscopy, fluorescence microscopy

1 | INTRODUCTION

Viruses are intercellular, obligate parasites of different shapes and structures with genetic materials (DNA or RNA), and consist of a protein-coat or envelop for protecting the genetic material. They are known to exist in the helical, icosahedral, viral core, or asymmetrical conformations (Kuznetsov & McPherson, 2011). Coronaviruses (CoVs) belonging to the family *Coronaviridae*, are a large group of viruses primarily known to cause respiratory, enteric, neurological, and hepatic diseases of varying

severity in humans, mammals, fishes, and birds (Woo et al., 2006). The International Committee for Taxonomy of Viruses (ICTV) has classified coronaviruses into four major genera: α -coronavirus, β -coronavirus, γ -coronavirus, and δ -coronavirus. The Human CoV (HCoV) are positive-sense single-stranded RNA (+ssRNA) viruses with currently six of them reported. It includes α -coronaviruses (HCoV-229E, HCoV-NL63), β -coronaviruses (HCoV-OC43), HCoV Hong Kong University 1 (HCoV-HKU1), severe acute respiratory syndrome coronavirus (SARS-CoV), and Middle-East respiratory syndrome coronavirus (MERS-CoV). The

γ -coronavirus and δ -coronavirus mainly infect birds, fishes, and few animals (Pillaiyar, Meenakshisundaram, & Manickam, 2020). Although the identification of these viruses dates back to about 60 years, their prominence intensified with the epidemic outbreak of SARS-CoV in 2002/2003 surfaced from southern China. With 8,096 SARS affected cases and 774 deaths were reported to the World Health Organization (WHO), the fatality rate was estimated to be 9.6% (Chang, Yan, & Wang, 2020; WHO, 2014). After that, another epidemic outbreak was recorded in 2012 due to an analogous virus MERS-CoV that emerged in Saudi Arabia. It was observantly more fatal than the previous outbreak, claiming the lives of 858 out of the 2,494 laboratory-confirmed cases globally reported to WHO, reaching the mortality rate of 34.4% (Guarner, 2020; WHO, 2019; Zaki, Van Boheemen, Bestebroer, Osterhaus, & Fouchier, 2012). Although the fatality rate was high, MERS-CoV was contained due to the low intensity of person to person transmission (R_0).

On December 31, 2019 a new strain of CoV as reported by WHO, showing pneumonia-like symptoms detected in Wuhan, Hubei province of China. Later it was identified as SARS-CoV-2 after isolation on January 7, 2020. Further named as 2019 novel coronavirus (2019-nCoV; CDC, 2020) and condition termed as coronavirus disease-19 (COVID-19), this outbreak was announced as a "Public Health Emergency of International Concern" on January 30, 2020 and declared as a pandemic by WHO on March 11, 2020, due to the speed and scale of transmission. Till March 20, 2020, a total of 234,073 confirmed cases and 9,840 deaths due to COVID-19 were reported to WHO worldwide (WHO, 2020). The rate of increase was rather abrupt, with 100,000 cases registered over the initial 3 months, and new 100,000 cases reported within the next 12 days. Although the death rate remained very low (about 2–3%), the R_0 is very high, between 2.5 and 3 (Guarner, 2020). Thus, precautionary measures are to be taken immediately and seriously.

Understanding the structure of a virus is an important aspect of virological studies. The word "Corona" comes from Latin, meaning "crown" or "halo." One of the defining features of these RNA viruses is the presence of clove-shaped, dumbbell-shaped, or pear-like spiky

projections that looks like a crown (Li, 2016; Siddell et al., 1983). Coronaviruses, in general, have a nearly spherical structure and are moderately pleiomorphic (Masters, 2006). There are four important structural proteins associated with the virus namely, envelope (E) protein, spike (S) protein, nucleocapsid (N) protein, and membrane (M) protein (Figure 1) (Spaan, Cavanagh, & Horzinek, 1988).

Previous studies have shown that the S protein (150 kDa) is a fusion glycoprotein that facilitates the viral attachment to the host cell. This structure gives the crown-like characteristic feature to the virus and is also responsible for the hemagglutinin activity. M protein (25–30 kDa) is one of the most abundant structural protein and provides definitive shape to the virion particles (Liu & Inglis, 1991). E protein (25–30 kDa) triggers the assembly and release of the virus, and also contribute to viral envelop formation by interacting with M proteins. The N protein binds to the genetic material in a string type conformation. β coronavirus has hemagglutinin-esterase (HE) protein that aids the S protein-mediated cell entry and virus spread through the mucosa (Spaan et al., 1988). Coronavirus replication is initiated with the binding of virion particles to the receptors of the cells, further directing the translation of the viral genome in the cytoplasm and synthesis of membrane-bound proteins. These structural proteins incorporate into the endoplasmic reticulum (ER) and are transported to the ER-Golgi intermediate compartment (ERGIC). Later on, the encapsulation process occurs, leading to the budding of the clustered particles into the ERGIC, and producing viroid. These viroids are carried to the plasma membrane of the cells through the formation of smooth-walled vesicles or Golgi sacs (Masters, 2006). Microscopic techniques are conventionally practiced for bacterial and viral identification and classification. They are feasible for observing and confirming the presence of viral particles based on morphological characteristics. Oshiro, Schieble, and Lennette (1971) visualized coronavirus particles (LINDER strain) using transmission electron microscopy (TEM) (Figure 2) and analyzed the progression of this viral infection by infecting human fetal diploid lung (HFDL) cells with tissue culture infectious dose 50 (TCID50) of coronavirus. The virus particles were

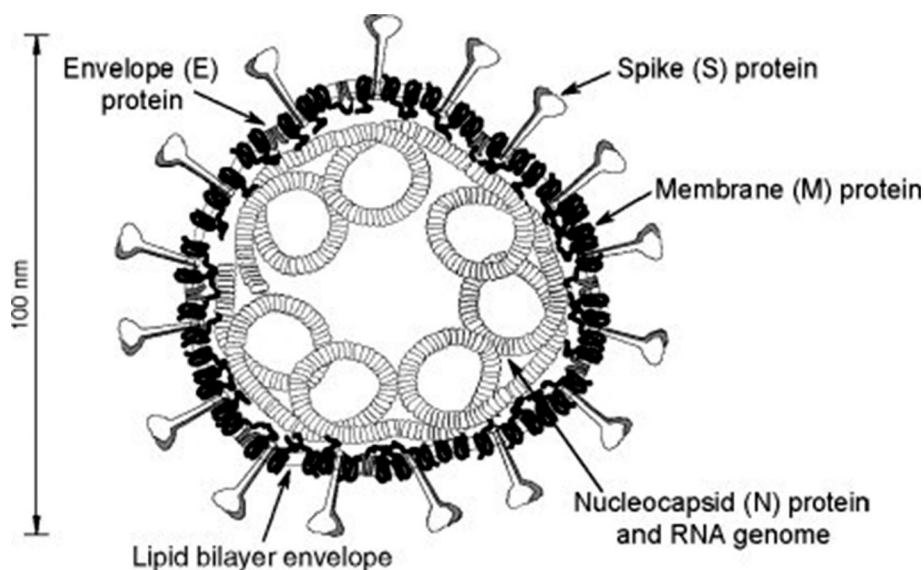


FIGURE 1 Schematic representation of coronavirus virion, displaying structural protein components. Source: This figure is adapted with permission from Masters (2006)

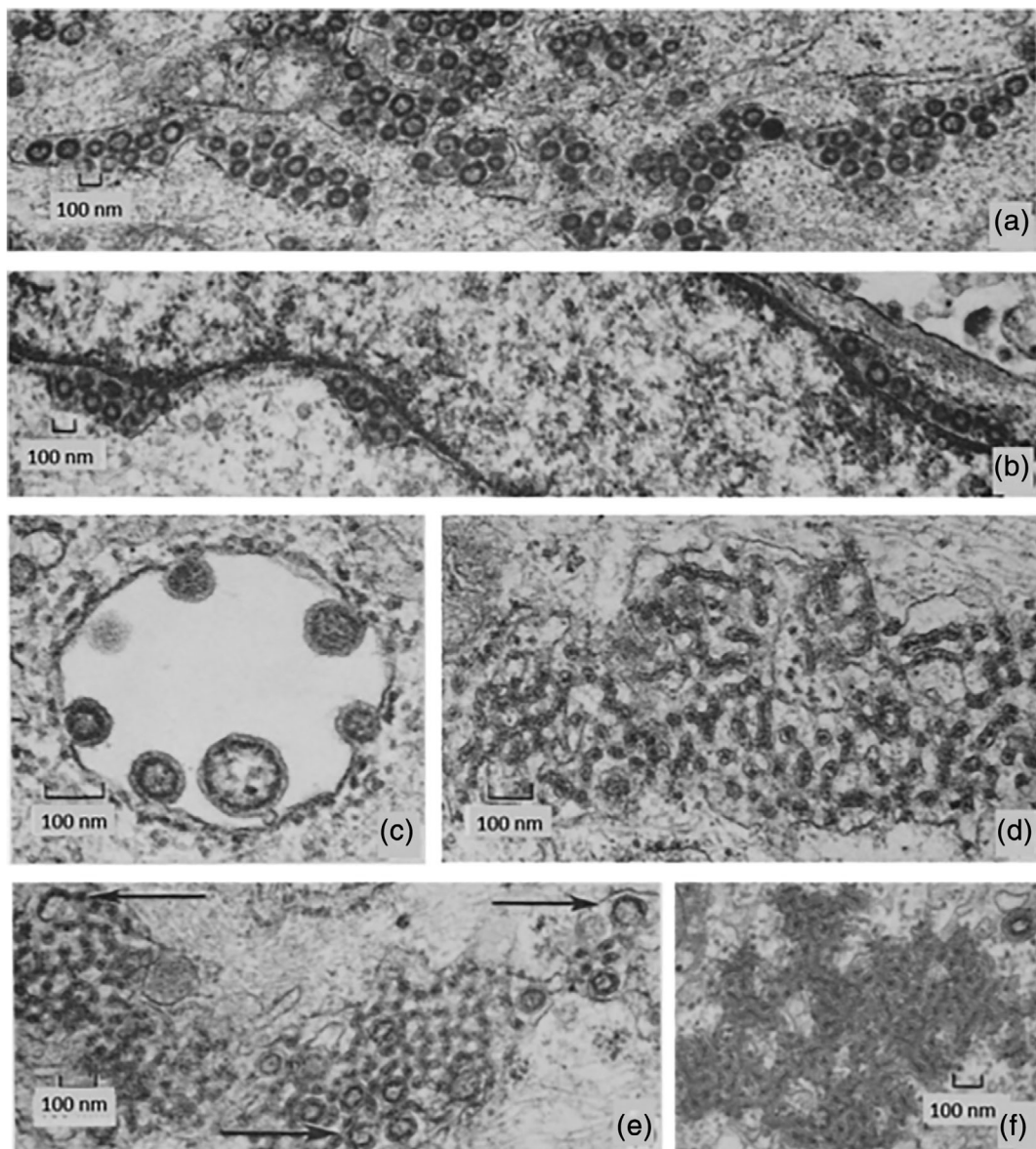


FIGURE 2 Thin-section electron microscopy images show the various development stages of coronaviruses in the human fetal diploid lung (HDFL) cells 24 hr after infection. Part figure (a) shows that coronaviruses are in the cisternae of the endoplasmic reticulum of a cell (part of cytoplasm). Part figure (b) shows that coronaviruses are in the perinuclear spaces in a cell. The virus particles are in spherical shape and its diameter ranges from 80 to 160 nm. Part figure (c) shows the formation of six particles inside a vacuole in the cytoplasm in various stages of budding process formation. Part figure (d) shows a tubular structure containing a dense material in cytoplasmic inclusion. Part figure (e) illustrates the relationship of virus particles to a cytoplasmic inclusion composed of tubular structures. Arrows in the figure point to structures of developing virus particles which also resemble the tubular structures of the inclusion. Part figure (f) shows that the cytoplasmic inclusion is composed of densely staining material around the tubular membrane. *Source:* This figure is adapted with permission from Oshiro et al. (1971)

found spherical of diameter ranges from 80 to 160 nm (Oshiro et al., 1971).

Previous studies have shown the use of a scanning electron microscope (SEM) for obtaining surface information and TEM for revealing inner components of the SARS-CoV particle. Also, their surface irregularities were investigated using atomic force microscopy (AFM). Recently, it was reported that 2019-nCoV (diameter of ~120 nm) can be easily identified under a TEM with its crown-like appearance, a

feature unique to coronaviruses (Monteil et al., 2020; Prasad, Potdar, Cherian, Abraham, & Basu, 2020). Accurate reconstruction of the viral particles can help to improve the understanding of science behind these viruses. Table 1 compares various microscopy techniques for understanding the structure of SARS-CoV and its effect in host cells. This review intends to provide an outline of various microscopic techniques used for investigating the structure and pathophysiology of coronavirus, as well as computational methods for the same.

TABLE 1 Different microscopic techniques and their significance in SARS-CoV studies

Microscopic technique	Principle	Significance in SARS-CoV study	Reference
Scanning electron microscope (SEM)	SEM uses a high energy electron beam to scan the sample surface and scattered electron from the sample surface is detected to obtain the image of the sample. Provides information about surface morphology and composition of a material. The acceleration voltage of electron: 40–120 kV. Instrument resolution: ~1 nm	Detection of the high resolution structure of the SARS-CoV	Lin et al., 2004; Akhtar, Khan, Khan, & Asiri, 2018
Transmission electron microscope (TEM)	In TEM, an electron beam is passed through the thin sample and transmitted electrons are detected. Reveals the internal composition of a material. The acceleration voltage of electron: 1–30 kV. Instrument resolution: ~0.1 nm	Morphological analysis of coronavirus (Linder strain) development isolated in human fetal diploid lung cells. Isolation and characterization of an oropharyngeal sample of a SARS patient revealed microstructural features of the corona virus. Detection of SARS-CoV-2 by direct throat swap specimen revealed the presence of stalk-like projections ending in round peplomeric structures	Oshiro et al., 1971; Akhtar et al., 2018; Ksiazek et al., 2003; Prasad et al., 2020; Williams & Carter, 1996
Cryo-electron microscope (Cryo-EM)	A thin layer of flash-frozen sample is scanned using low energy electrons to get a 2D image of the sample. Resolution: ~3.4 Å	3D reconstruction of the HCoV-NL63 spike glycoprotein trimmer	Walls et al., 2016; Baker, 2018
Atomic force microscope (AFM)	AFM works by scanning the sample surface with a cantilever probe to which a LASER is pointed to measure surface variations. Working modes—tapping mode, contact mode, and noncontact mode. Resolution: ~ up to 30 nm	Study the surface ultrastructure of SARS-CoV. Observe the changes in the cell membrane during the release of a virion particle. Study the absorption of SARS-CoV viral particles in biopolymeric vesicles. To study the structure and size of spike proteins which is present in the viral coat	Yang, 2004; Lin et al., 2005; Eaton & West, 2010; Ng et al., 2004; Ciejka, Wolski, Nowakowska, Pirc, & Szczubiałka, 2017; Lee et al., 2004
Fluorescence microscope (FM)	FM detects the fluorescence emitted by fluorophore when excited with the specific absorption wavelength. The fluorophore binds to the object of interest. The object is seen against a black background which provides high contrast. Fluorescence source: LASER, LED, etc. Spatial resolution of confocal fluorescence ~ up to 250 nm	Study the endocytosis pathway involved in SARS-CoV entry into cells. Understand the role of lipid raft for virion entry into the cell. Determine the antigenic morbidity present in SARS-CoV which gives rise to an immune reaction. Investigate cell cycle arrest induced by SARS-CoV in G0/G1 phase. To show the localization of viral proteins within Golgi complex and endoplasmic reticulum during SARS-CoV infection	Diaspro, 2010; Diaspro, 2010; Lichtman & Conchello, 2005; Wang et al., 2008; Lu, Liu, & Tam, 2008; Manopo et al., 2005; Yuan et al., 2006; Yuan et al., 2005; Knoops et al., 2008

2 | ELECTRON MICROSCOPY VISUALIZATION OF SARS-COVs

Electron microscope (EM) uses an accelerated beam of electrons as the source of illumination to attain higher magnification and resolution up to a few nanometers of particle size, making them favorable for viral studies and diagnosis. The visualization and characterization of viruses

have become easier with the intervention of EM in biology. EM played a crucial role in characterizing the causative virus during the SARS outbreak in 2002/2003 (Goldsmith & Miller, 2009; Lin et al., 2004) and the ultra-high resolution SEM was able to visualize the SARS-CoV in three-dimensional (3D) with 10–20 nm spikes on the virion surface.

The initial identification of coronavirus during the 2003 outbreak has relied on tissue culture isolation followed by EM visualization. The

novel coronavirus that was successfully isolated from patients with SARS and identified them using TEM. The oropharyngeal sample from the patient was inoculated into Vero E6 mammalian cell lines (Ksiazek et al., 2003). The E6 cell lines were subjected to thin-layer electron microscopy and the images revealed typical coronavirus particles within the rough endoplasmic reticulum, specifically in cisternae, as well as in vesicles and several large clusters of extracellular particles were found attached to the surface of the plasma membrane. Negative-stain electron microscopy images of these particles have elucidated that the virus particle dimensions were within the diameter range from 80 to 140 nm and the surface projections with the length between 20 and 40 nm. The SARS-CoV exhibit similar morphological characteristics as other members of their family *Coronavirida* when observed under TEM. The viral nucleocapsids form new particles that are lined along the membranes of the rough endoplasmic reticulum (RER) and the Golgi complex. The envelop formation of virions occurs in this membrane region and is majorly spherical, sometimes pleomorphic in shape. Surface projections or the spikes can be indistinctly observed in the thin-sections. The virus particles were observed in membrane-bound vesicles, either individually or in clusters. Tubular structures with an average diameter of 20 nm, are also seen within the vesicles (Figure 3). The infected cells have many empty vesicles and fewer mitochondria compared with normal cells. Further, the outer membrane and crista of mitochondria appear to be disturbed. Endoplasmic reticula look swollen and remaining organelles are hardly seen. The chromatin in the nucleus shrink and assemble along the margin, with a rare appearance of some tiny granules in the nucleus. However, in normal cells, there are less empty vesicles and mitochondria which are undamaged. They gradually move toward the cell surface and fuse with the plasma membrane from where the viral particles are released. The aggregation of particles in the plasma membrane can be viewed as a "knob-like structure" on the cell surface (Goldsmith et al., 2004).

These SARS-CoV particles have a typical crown structure and a single virion is surrounded by 15 spike protein (Lin et al., 2005). They tightly adhere through their projections sticking into each other, and thus form a mosaic patch and leading to the compression of the virions. These flower-shaped projections corresponding to the spike are the main constituent of S protein, have a size ranging from 10 to 20 nm. It was possible to observe the projections with a regular structure composed of three subunits, like a flower with three petals (Lin et al., 2004) (Figure 4). Semi-thick sections (100 nm) of cryofixed SARS-CoV-infected Vero E6 cells were observed through TEM (Figure 5) to investigate the membrane structure alterations in the host cell. It was found that RNA synthesis in this virus is associated with the formation of double membrane vesicles (DMVs). These DMVs are interconnected through the outer membrane and form a huge network that is continuous with the rough ER. The DMVs are 8 nm in diameter with "neck-like" connections to other DMVs and cisternae of the RER (Knoops et al., 2008).

HCoV-NL63 is an α -coronavirus causing severe lower respiratory tract infections. High-resolution cryoelectron microscopy was used to reconstruct the spike glycoprotein trimer of the virus which is

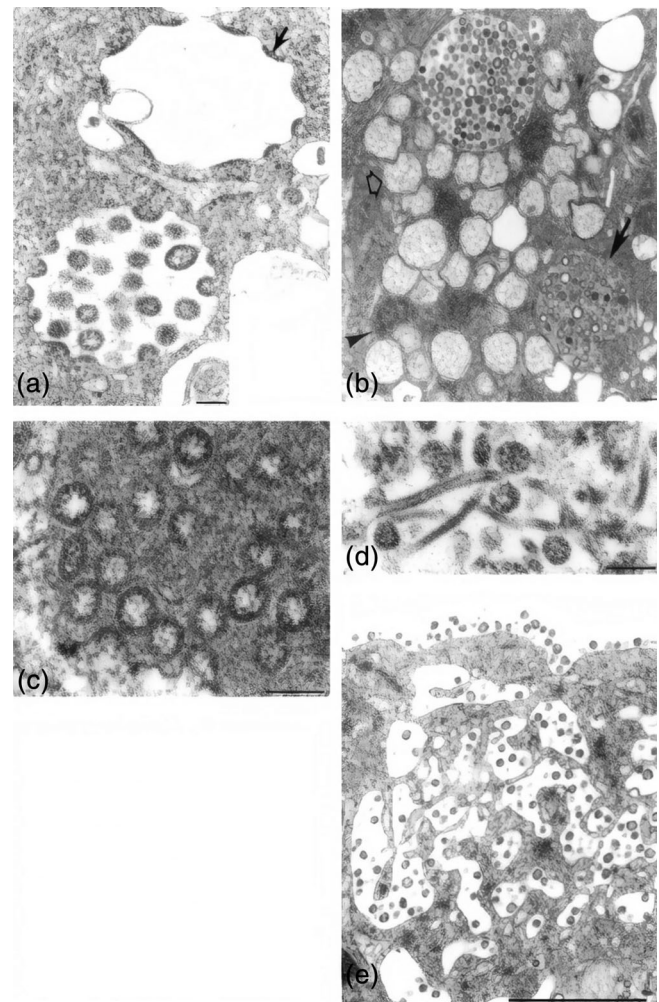


FIGURE 3 Assembly of SARS-CoV particles in host Vero E6 cells. (a) Depicting nucleocapsids (arrow) measuring 6 nm in diameter along membranes of the budding compartment are viewed in cross-section. Pretreatment with Tannic acid improves the visibility of the club-shaped viral projections with an average length of 14 nm (inset). (b) SARS-CoV-infected cell with virus-containing vesicles of granular material interspersed among the virions (arrow), double-membrane vesicles (open arrow), and nucleocapsid inclusions (arrowhead). (c) Virus-containing vesicle with dark granular material observed at higher magnification. (d) Tubular structures in a virus-containing vesicle. (e) Migration of virions in vesicles toward the plasma membrane and its fusion with it. The characteristic lining of particles along the cell surface is observed. Bars: (a), inset; (b–d), 100 nm; (e), 1 μ m. Source: This figure is adapted with permission from Goldsmith et al. (2004)

responsible for entry into host cells and neutralizing antibodies produced by the body during infection. It is suggested that HCoV-NL63, HKU1, and other coronaviruses may use a molecular trickery mechanism that involves covering or hiding the epitopes with glycans and triggering conformational changes, to dodge the immune system of hosts which has been elucidated by cryoelectron microscopy (Walls et al., 2016). Thus, EM including SEM as well as TEM is very useful in investigating the structure of coronavirus with a high spatial

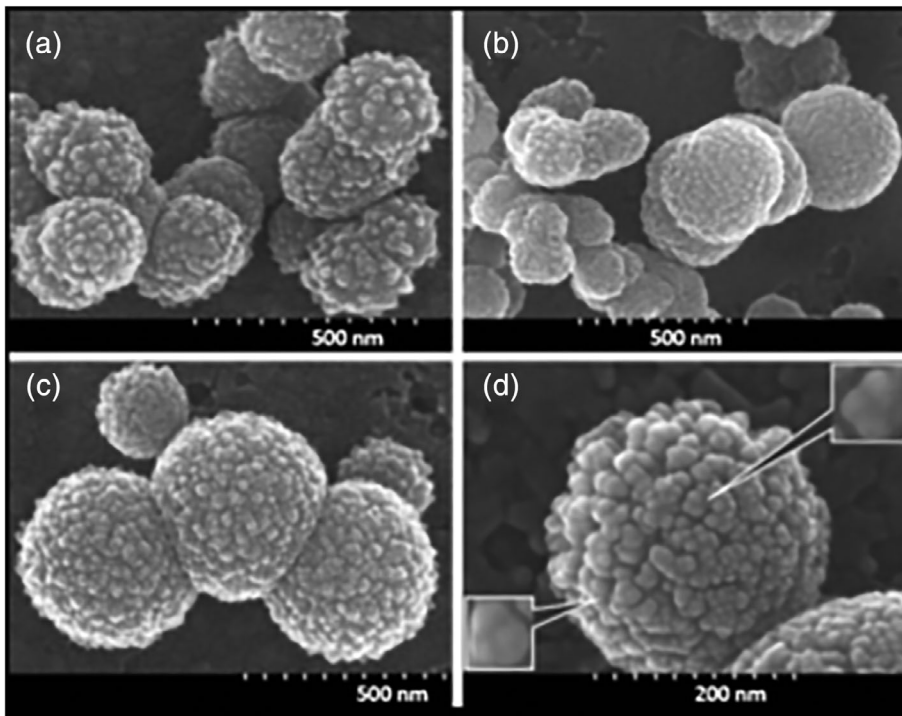


FIGURE 4 Shows the virions with a diameter of (a) 200, (b) 100 and 200 nm, and (c) 400 nm. (d) The ultrastructure of the surface projections. Two typical spikes are magnified to show the trimer structure (insets). *Source:* This figure is adapted with permission from Lin et al. (2004)

resolution which further leads to understanding its development and effect in the host cells. Also, microscopic characterization of the trimeric structure of spikes contributes to the development of future antiviral strategies.

3 | VISUALIZATION OF SARS-COV5 BY ATOMIC FORCE MICROSCOPY

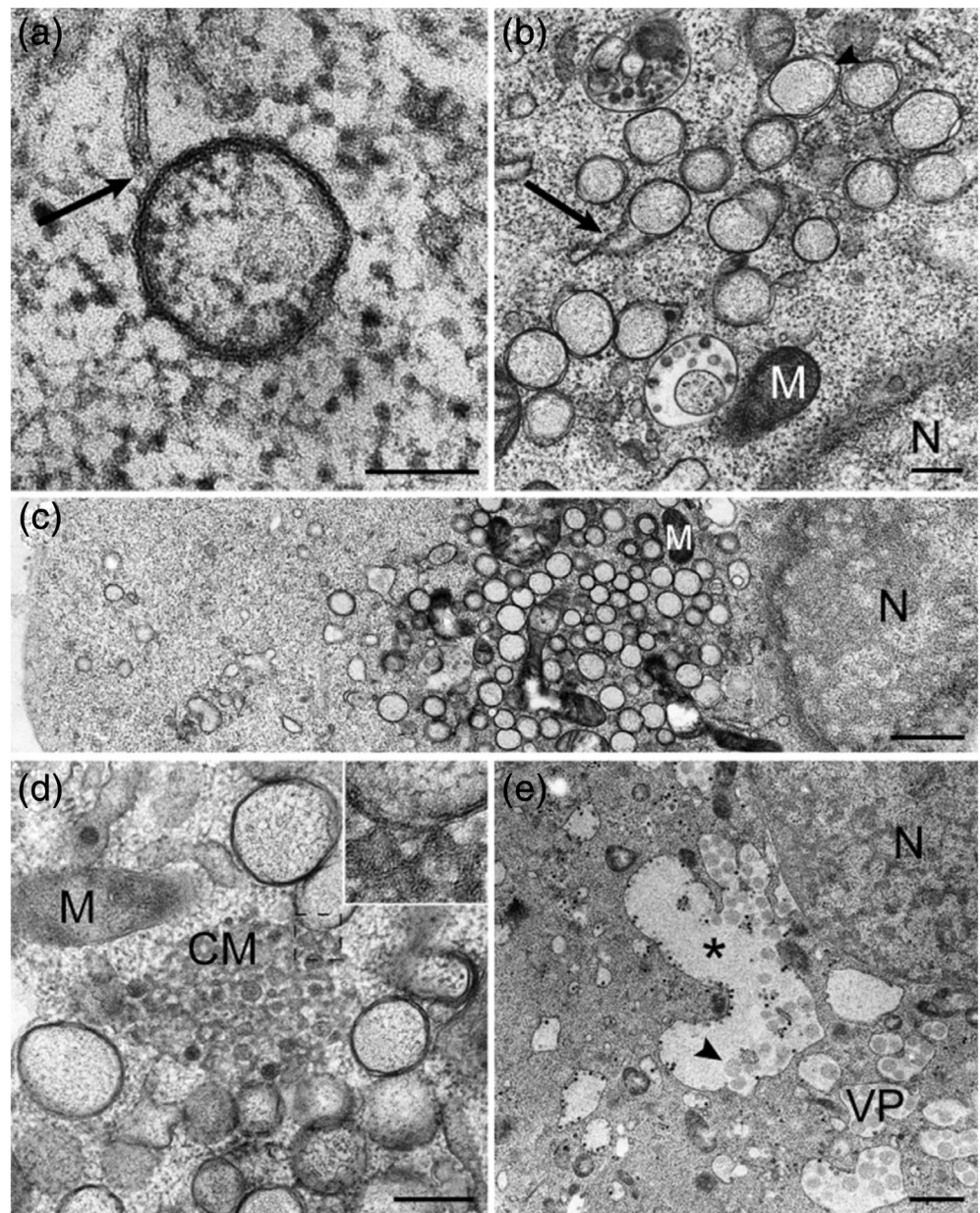
The AFM is primarily used in the field of material sciences after its invention in 1986 (Eaton & West, 2010). The emphasis of AFM in biology surged about a decade later, due to its efficacy in studying wide ranges of biological materials such as cells, macromolecules, proteins, and nucleic acids (Parot et al., 2007). It has become an important tool to investigate surface topologies in life sciences research including cell morphology, tissue heterogeneity, bacterial and viral characteristics, and structure identification (Yang, 2004). One of the advantages of using AFM is the atomic and molecular resolution achieved which is close to that obtained by an EM (Lin et al., 2005). It can also be used for revealing the inner architecture by scanning the internal layers using chemical, physical, or enzymatic methods to expose the interior of the viruses. These applications have proved AFM to be an important tool in virology.

AFM has been used to study morphology as well as surface structure of viruses like the influenza virus, herpes simplex virus, and tobacco mosaic virus (Drygin, Bordunova, Gallyamov, & Yaminsky, 1998; Epan et al., 2001; Plomp, Rice, Wagner, McPherson, & Malkin, 2002). SARS-CoV, a highly pathogenic virus exhibits structural prominence with the presence of crown-like structures surrounding them as mentioned earlier and can also be

visualized under AFM to investigate the ultrastructure of the virus along with cell to cell transmission. The surface ultrastructure of SARS-CoV was studied using AFM. The virus particles appeared spherical with protrusions, on the surface of micato which they were attached electrostatically for the study. Single virions were selected from the AFM images and root mean square (RMS) value of heights of virion particles was found to be 81.2 ± 10.6 nm as shown in Figure 6. The presence of crown-like surface structures was confirmed using high-resolution AFM images by analyzing the surface organization of the single virion before and after treatment with hydroxyoctanoic acid and protease, respectively. The phase images of the surface showed different hard and soft regions. The decrease in surface height after treatment confirmed that surface particles were proteins. To further verify that the spherical surface particles were spike protein, immunoglobulin G (IgG) having the same molecular weight as spike proteins (~ 150 kDa) were imaged by AFM and compared with the protein. The AFM IgG height obtained was same as the surface bumps speculated as spike protein. The AFM images also showed that a virion contains about 15 spike proteins on the surface (Figure 6d) which indicated the feasibility of using AFM for imaging SARS-CoV particles (Lin et al., 2005).

Further, the maturation and release of SARS-CoV from the infected cell were studied. Both SEM and AFM were used to understand the surface changes of the Vero E6 infected host cells with SARS-CoV, which was grown on coverslips. AFM imaging revealed that there was the localized breaching of the plasma membrane due to the fusion of vacuoles carrying the virions, which facilitated the virus particles to move out of the cells as shown in Figure 7. The crown appearance of the SARS-CoV virions, confirmed by 3D reconstruction of AFM images, appeared to be shorter than other

FIGURE 5 Membrane alterations observed in Vero E6 host cells infected with SARS-CoV under TEM. (a) Early double-membrane vesicle as observed in a few sections, showing a connection (arrow) to a reticular membrane. (b) Clusters of DMVs began to form and arrows depicting connections between the outer membrane of DMV and reticular membrane structures (arrow). Arrowhead depicts luminal spacing between the outer and inner membrane of DMV. (c) Image shows the DMVs were concentrated in the perinuclear region (nucleus; N), often mitochondria (M) present in between. (d) The cluster of CM surrounded by groups of DMVs where these structures are continuous with the DMV outer membrane (inset). (e) During the later stages of infection, DMVs appeared to merge into VPs, resulting in developed large cytoplasmic vacuoles (asterisk) that contains single-membrane vesicles (arrowhead pointing to an example) and budding virus particles. Scale bars are 100 nm (a), 250 nm (b and d), or 1 μ m (c and e). *Source:* This figure is adapted with permission from Knoops et al. (2008)



coronavirus species. Subcellular examination enumerated that there was thickening of cell periphery in the case of infected cells. This modification was supported by the deposition of actin filaments which made the cell surface puffy providing the force for outward transport of virus particles (Ng et al., 2004). Apart from the structural analysis of the virus, AFM was used to study the adsorption of virus particles in biopolymeric vesicles. The biopolymer was used to concentrate the virions quantity for various biological experiments as well as for purification of virus-contaminated water. After the initial adsorption quantified using reverse transcriptase-quantitative polymerase chain reaction (RT-qPCR), AFM was used to confirm that the virus particles were successfully attached to the biopolymer. AFM images revealed densely distributed particles approximately 140 nm (diameter) on the surface which were absent in the case of untreated vesicles (Ciejka et al., 2017).

Hence, AFM studies on coronavirus have provided substantial evidence on the efficiency of the technique for imaging and identifying coronavirus specifically. The present pandemic 2019-nCoV exhibits characteristic features very similar to that of SARS-CoV, thus the findings of these studies can be extended for revealing more information and further improve our understanding of 2019-nCoV.

4 | FLUORESCENCE MICROSCOPY OF SARS-COVs INFECTED CELL

Fluorescence microscopy is one of the mainstays for imaging various biological components and systems with high selectivity and specificity. In this technique, the object of interest is highlighted with various fluorescence probes and viewed in the dark background providing better

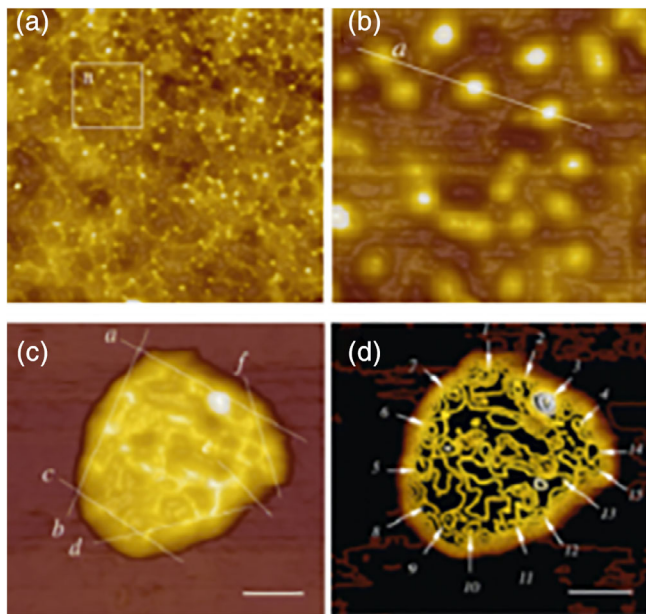


FIGURE 6 Topographic two-dimensional (2D) AFM images of the (a, b) native SARS-CoV particle on mica of scanning areas are 10 and 2 mm² for the low- (a) and high-resolution (b) images, respectively. Part figure (b) is the zoomed image of the box areas is displayed in (a) reveals the presence of SARS-CoV particles. (c, d) 2D AFM image and contour map of single SARS-CoV virion. Scale bar = 100 nm. The corresponding cursor profiles (middle and bottom row) provide quantitative measurements of the dimensions for the spike proteins (1–15) displayed in (d). *Source:* This figure is adapted with permission from Lin et al. (2004) [Color figure can be viewed at wileyonlinelibrary.com]

contrast (Diaspro, 2010). With the rapid development of the fluorescence technique, various modern microscopies such as laser scanning confocal microscope and superresolution microscopes are used mainly for biomedical applications due to less destructive process as compared with an electron microscope (Lichtman & Conchello, 2005). Fluorescence microscopy has been used for investigating viruses and their interactions in cellular systems (Beilstein et al., 2019; Dáder et al., 2019; Kumar et al., 2017; Mazumder et al., 2013; Zgheib et al., 2019). SARS-CoV is a highly contagious virus and various pathological facet of the virus yet unknown.

The virus was initially thought to enter the cell either by fusing with the plasma membrane but later studies showed that viral entry also involves endocytosis (Sieczkarski & Whittaker, 2002). In a study, confocal fluorescence microscopy was used to investigate the endocytic pathway by the virus and found SARS-CoV enters HEK293E cells through pH- and receptor-dependent endocytosis. SARS-CoV functional receptor angiotensin-converting enzyme 2 (ACE2) was labeled with GFP by the transfection of HEK293E cells. Treatment of HEK293E cells with SARS-CoV spike protein resulted in the translocation of the ACE2, from the cell surface to its endosomes. The translocation of the ACE2 receptor was observed under a confocal fluorescence microscope on the HEK293E-ACE2-GFP cells proving the endocytosis-based entry of the virus into the cells (Figure 8a) (Wang et al., 2008). Due to this endocytic entry, the cellular rate of infection of the virus

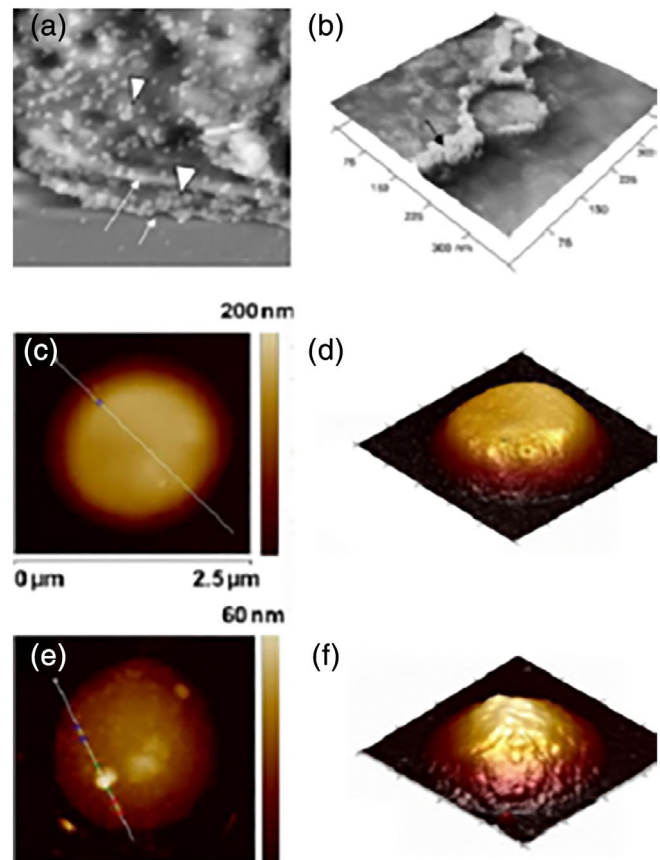


FIGURE 7 (a) Shows the AFM image of the thickened, layered appearance of the edge of Vero cells infected with the severe acute respiratory syndrome-associated coronavirus (arrows), where active virus extrusion occurs. Arrowheads indicate the virus particles. (b) Represents the 3D AFM image showing SARS-CoV extruding out from infected Vero cell. The arrow indicates the thickening of the cell membrane observed during this process. *Source:* This figure is adapted with permission from Ng et al. (2004). (c–f) The nano/microspheres of N-(2-hydroxypropyl)-3-trimethyl chitosan (HTCC-NS/MS) bind HCoV NL63 virions. Height and 3D AFM topography images of H-HTCC-MS incubated with lysate of mock-infected (c) or virus-infected (e) cells. The scan size is 2.5 × 2.5 μm for the 2D image. Scan size and the vertical scale on 3D figures: 2.5 × 2.5 μm and 100 nm (c); 2.0 × 2.0 μm and 50 nm (e), respectively. *Source:* This figure is adapted with permission from Ciejka et al. (2017) [Color figure can be viewed at wileyonlinelibrary.com]

has shown to be increased. This finding also contributes to understand the pathogenesis of the virus and may lead to antiviral drug research.

The above study also pointed out that lipid rafts play an important role in endocytosis of the SARS-CoV. Further, the involvement of lipid rafts in SARS-CoV entry into the Vero E6 cell was studied. Lipid rafts are domains that concentrate membrane-associated proteins including receptors and signaling molecules including ACE2 receptors. The confocal fluorescence images (as shown in Figure 8b) showed the co-localization of ectodomain (S1188HA) spike protein with raft-resident ganglioside GM1 and hence lipid rafts play a significant role. Thus, proving that SARS-CoV requires intact lipid raft for entering into the host cells (Lu et al., 2008).

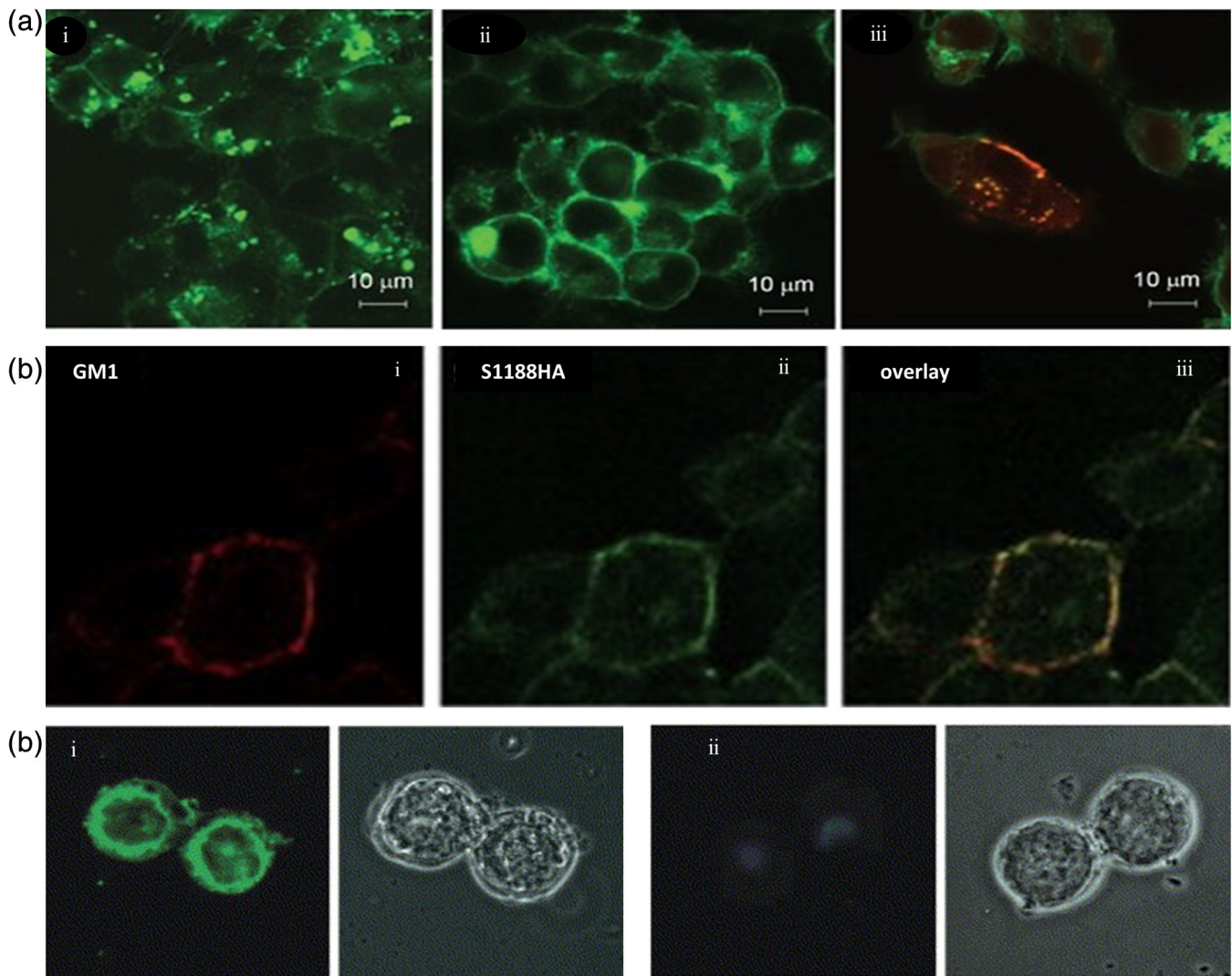


FIGURE 8 (a) Endocytosis mediated entry of SARS-CoV spike-bearing pseudoviruses into the cell; (i) image shows the translocation of the ACE2 receptor when the HEK293E-ACE2-GFP cells were treated with spike-bearing pseudovirus, (ii) image shows the absence of translocation of the ACE2 receptor when the HEK293E-ACE2-GFP cells were treated with spike-minus pseudovirus, and (iii) shows the co-localization of the spike protein and ACE2-GFP in cytoplasmic vesicles showing a viral entry. *Source:* This figure is adapted with permission from Wang et al. (2008). (b) The confocal fluorescence image showed the colocalization of spike protein with lipid raft; (i) shows the raft-resident ganglioside GM1, (ii) image shows SARS-CoV S protein, and (iii) merged image, enumerating the interaction of the viral protein with lipid raft. This figure is adapted with permission from Lu et al. (2008). (c) Immunofluorescence assay based on spike protein containing the Sf-9 cells bearing the protein C domain; (i) when treated with virus-infected human serum shows the presence of fluorescence and (ii) image shows the absence of fluorescence ring when treated with normal human serum. *Source:* This figure is adapted with permission from Manopo et al. (2005) [Color figure can be viewed at wileyonlinelibrary.com]

Apart from studying how the virus enters the cell, immunofluorescence was also used to investigate antibody response to the SARS-CoV and use it as an efficient detection method. A 441–700 amino acid domain (called the protein C) representing the S1 of the spike protein was identified to be responsible for the immune response. Protein C domain expressing baculovirus was allowed to infect *Spodoptera frugiperda* (Sf-9) cells and the cells were fixed on coverslips (forming the antigen part of immunoassay). It was found that there was fluorescence ring around the Sf-9 cells which were treated with virus-infected serum but was absent when treated with normal human serum as shown in Figure 8c. This proved that, protein C gives rise to an immune reaction. There was a clear difference between the spike

protein based-immunofluorescence assay (IFA) and commercial IFA in terms of the fluorescence signal when observed under an inverted fluorescence microscope improving the specificity and sensitivity of the conducted IFA (Manopo et al., 2005).

Immunofluorescence-based analysis was also used to investigate the 7a protein in SARS-CoV which is responsible for arresting the infected cell's cycle at G0/G1 phase. The 7a protein was cloned into pCMV-myc vector and transfected in HEK 293 cells. Flow cytometric analysis showed that HEK 293 cells infected 7a/pCMV-myc grew slower than the ones only with pCMV-myc. Further SARS-CoV 7a tagged GFP was cloned and allowed to infect HEK 293 cells. This also showed that the 7a-GFP positive cells had lesser incorporation of

BrdUrd than the 7a-GFP negative cells indicating that cells are being obstructed from entering the S-phase. It was also established that G0/G1 arrest is not an apoptotic inducer in SERS-CoV infected cells. The study also concluded that the cell cycle arrest was via cyclin D3/Rb pathway (Yuan et al., 2006). SARS-CoV has shown the presence of various non-structural proteins between the S and E genes or the M and N genes and may differ from species to species of the virus. Among the five nonstructural proteins with more than 50 amino acids are in the intergenic regions, SARS 3a (ORF 3) is expressed in the SARS-CoV infected cells. It was found that the SARS 3a protein is important for the viral life cycle and is found to localize within the Golgi complex and plasma membrane of the infected cells and is also an integral membrane protein of the phospholipid bilayer. Confocal fluorescence microscopy assisted in studying the colocalization of 3a with the M protein in the Golgi complex of infected cells (Yuan et al., 2005). Further, being a positive-stranded virus, the replication of SARS-CoV is linked with a synthesis of the negative strand of the genome which leads to the formation of various ds structures. Vero E6 cells were infected with SARS-CoV virus and incubated with an antibody specific for the dsRNA. It was observed that the fluorescence from ds RNA started appearing 2 hr after the infection and the same was observed located close to the nucleus during the later stage of infection. Thus, indicating that the replication of SARS-CoV is associated with the endoplasmic reticulum. Co-labeling of nsp-3 or -8 (nonstructural protein) responsible for RNA replication, showed its close association with the dsRNA (Knoops et al., 2008).

Most of the above studies have shown how the virus infects the host cell and the various proteins associated with the infection process. However, SARS-CoV being an RNA virus, the entry of genetic material into the cell, and getting integrated into the host genome is also essential to understand its pathogenesis. Recently, the possibility of imaging a single RNA molecule inside the Cos-7 cells was shown with the fluorogenic Mango II arrays. The array was found to have a better signal to noise ratio than existing RNA markers and can be used to track a single RNA molecule for an extended period. The array can be used for SARS-CoV related studies to investigate the integration of RNA in infected cells, and provide deeper insight into the pathology of the virus (Cawte, Unrau, & Rueda, 2020).

Thus, fluorescence microscope though limited by its spatial resolution to study the ultrastructure of the SARS-CoV, has been used to understand how the virus infects cells and finds the various domains of the virus which are essential for its infection. It also helped us to understand the localization of various viral particles and protein at the cellular and subcellular location; and with further development of fluorophores, the movement of viral genetic material after infection can be observed.

5 | COMPUTATIONAL STUDIES OF SARS-COVs

Even though the outbreaks of SARS (2003) and MERS (2012) led to global alert by WHO, there are no approved drugs yet to treat this

deadly coronavirus. The recent pandemic outbreak of the 2019-nCoV needs to be immediately addressed effectively with an alternative therapeutic solution as we are experiencing high rates of global mortality. In the future, emerging coronaviruses will still be a global threat to public health. Thus, narrowing down a wide range of inhibitors to decrease the effects of coronavirus infection is challenging and the computational approach contributes to overcome this challenge. Bioinformatics and computational biology should be utilized to achieve the aforementioned need as it involves cost-effective and faster approaches. Therefore, in this section, we present various approaches and strategies reported to understand the 2019-nCoV.

To start with, the genome sequence of the 2019-nCoV was first released to the public domain on January 12, 2020 by WHO. There on, several coronavirus whole genomes were sequenced around the globe. Analysis of these suggested that it was similar to bat SARS-like-CoVZXC21 with 89% identity and to human SARS-CoV with 82% identity. On the construction of phylogenetic trees, it was observed that proteins of 2019-nCoV such as spike glycoproteins, membrane proteins, orf1a/b, small envelope proteins, and nucleoproteins were closely associated with the bat, and human coronaviruses (Chan et al., 2020). In the third week of January 2020, Cleemput et al. stated that the Genome Detective Coronavirus Typing tool was used for the characterization of 2019-nCoV infections by analyzing viral genomes within a short time. Multiple FASTA sequences can be submitted at once, which are queried against reference sequences using dynamic aligner and annotated genome aligner (AGA). It was used for the identification of viral species and spotting mutations in viruses (Cleemput et al., 2020). Again, evolutionary studies were performed by constructing phylogenetic trees from the genome sequences and this analysis also reported the close association of 2019-nCoV with SARS-CoV, and Bat-CoV. The phylogenetic profiling reported that two non-structural proteins, NS7b and NS8, were conserved among 2019-nCoV, BatSARS-like CoV, and BetaCoV_RaTG. Thus, it was inferred that the functional changes in these proteins may be responsible for the infective property of 2019-nCoV (Fahmi, Kubota, & Ito, 2020). Also, the phylogenetic analysis result of coronaviral S protein showed the closest distance of evolution between MERS-CoV and HCoV-OC43 in terms of structure and sequence. Both MERS-CoV and HCoV-OC43 are very contagious. Results of network analysis explained the interaction between human IC1 protein and SARS-CoV proteins. It was reported that IC1 protein affects the activation of the complement system and nonstructural proteins of SARS-CoV. This indicated that the virus affecting the host immune proteins may also affect the normal immune process (Kim, Cho, Lee, Kim, & Son, 2019). Further, it was presented that nCoV-2019 and the closest Bat relative exhibited identities of more than 85% along with the fully conserved genome (~30 kb) (Ceraolo & Giorgi, 2020). It was also reported that humans possessed two T and B cell epitopes from Betacoronaviruses and 398 from SARS-CoV. For B cell epitopes, Discoptope prediction was used and algorithms were used for T cell epitopes. B and T cell epitopes were observed to be conserved between 2019-nCoV and SARS-CoV based on phylogenetic analysis (Grifoni et al., 2020).

To obtain information based on the molecular level of structures of 2019-nCoV proteins and their function, computational predictions were used in addition to various experimentally solved structures. In 2016, Kirchdoerfer et al. reported that N-terminal domain of the spike glycoprotein subunit 1 of SARS-CoV was modeled using Modeller, a homology tool presents in UCSF Chimera, where bovine CoV NTD with PDB ID-4H14 was used as a template. The modeled structure was docked with Human Coronavirus I (HKU1) and refined using Rosetta. Clustering was performed on refined models dependent on pairwise RMSD. A model with the least energy was chosen for further refinement (Kirchdoerfer et al., 2016). Along with this model, C-Terminal Domain from SARSCoV with PDB ID-2AJF was used to build and refine the model. The available

structure of the target gene Mpro (Main protease) was used to identify potential drugs for 2019-nCoV using molecular docking and the results of this study confirmed the earlier preliminary reports that some of the drugs approved for other viral infections can be used to treat 2019-nCoV infections (Talluri). Another study also focused on the same drug target, the main protease (Mpro, 3CLpro), and structures of 2019-nCoV Mpro and its complex with an α -ketoamide inhibitor (Figure 9a) were used in this study. The characterization of α -ketoamide based on its drug-likeness, ADME and toxicity properties reveals that it can be administered by inhaling (Zhang et al., 2020).

Recent studies have identified Human Angiotensin-Converting Enzyme 2 (hACE2) as a potential receptor for interacting with spike

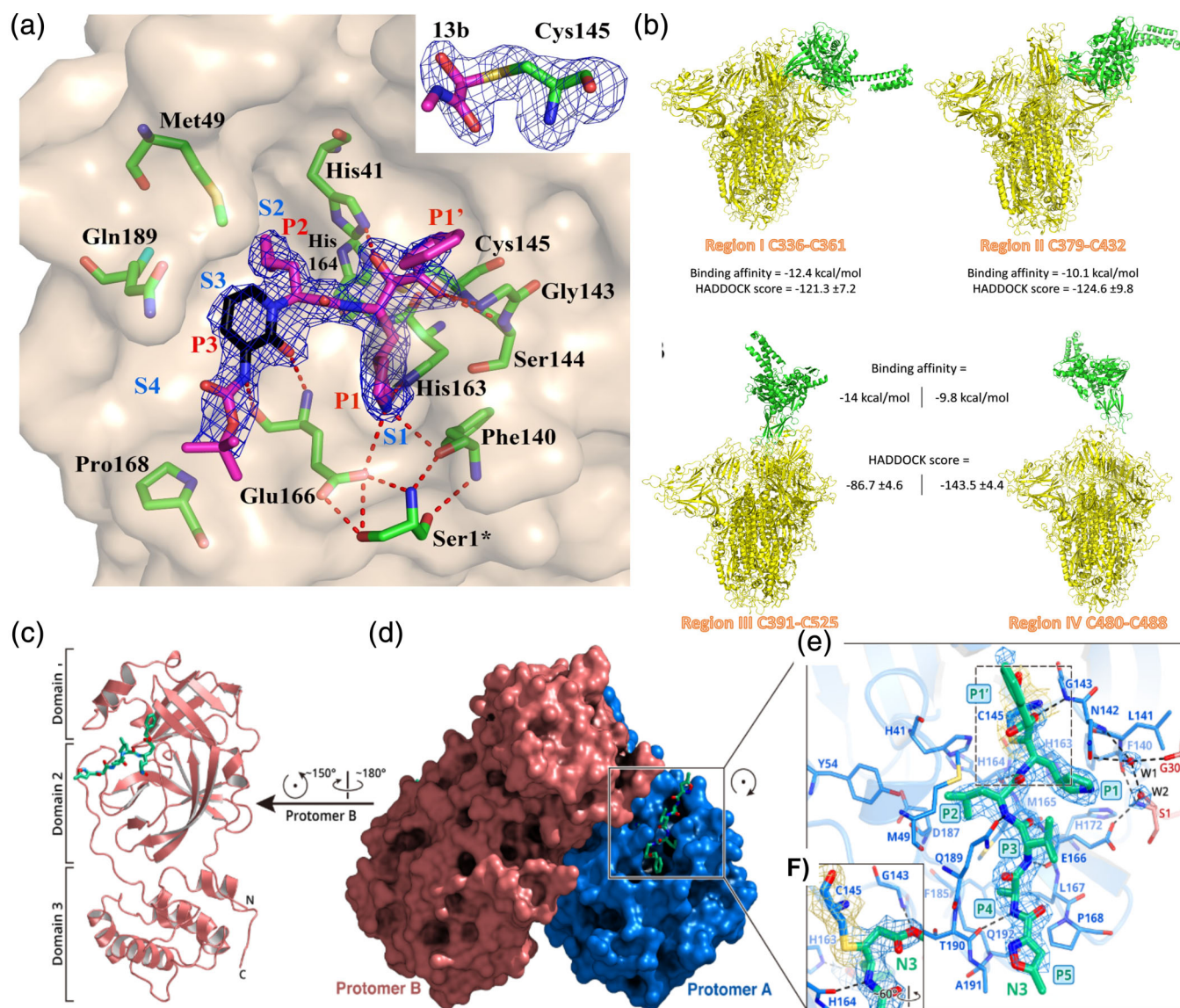


FIGURE 9 (a) Main protease interacting with the compound 13b at the binding cavity present between the two domains of Mpro. (b) The structure of the docking complexes of GRP78 represented in green and COVID-19 spike glycoprotein represented in yellow. (c) The crystal structure of COVID-19 Mpro in complex with N3 inhibitor. (d) Surface of target Mpro. (e) Binding cavity of Mpro and its key residues interacting with N3 inhibitor. (f) Zoomed in view of the interaction involving C-S covalent bond between the N3 inhibitor and the target Mpro. Source: This figure is adapted with permission from Zhang et al. (2020); Ibrahim, Abdelmalek, Elshahat, and Elfiky (2020); and Jin et al. (2020) [Color figure can be viewed at wileyonlinelibrary.com]

TABLE 2 Various tools and software used for SARS-CoV and 2019-nCoV computational studies

Name of the tool/software	Description	Type of license	Reference
RAxML	Sequential and parallel maximum likelihood based inference of large phylogenetic trees	Free web-based server	Fahmi et al., 2020
MEGA X	Analyze evolution and build phylogenetic trees	Freeware	Fahmi et al., 2020; Zhou et al., 2020; Chan et al., 2020; Wu, Liu, et al., 2020; Wu, Zhao, et al., 2020
MAFFT	Multiple alignment program	Free web-based server	Fahmi et al., 2020
CLUSTAL omega	Multiple sequence alignment tool	Free web-based server	Chan et al., 2020; Ibrahim et al., 2020
Clustal W	Progressive multiple sequence alignment	Free web-based server	Wu, Liu, et al., 2020; Wu, Zhao, et al., 2020
C-I-TASSER	Server for protein structure prediction using multiple threading method LOMETS	Free web server	Fahmi et al., 2020
Modeller	Homology modeling software for protein structure determination	Freeware/commercial	Kirchdoerfer et al., 2016
AutoDock Vina	Molecular docking program	Open source	Talluri,
ICM-dock	Docking software	Commercial	Wu, Liu, et al., 2020; Wu, Zhao, et al., 2020
HADDOCK	Performs flexible biomolecular docking	Freeware	Ibrahim et al., 2020
COVID-19 docking server	Dock ligands to COVID-19 targets	Free web-based server	Kong et al., 2020
VMD	Visualize and analyses molecular dynamics simulations	Freeware	Zhou et al., 2019
Nanoscale molecular dynamics	Charm++ parallel programming model-based simulation software	Freeware	Zhou et al., 2019
AGA	Performs local/global alignment	Free web-based server	Cleemput et al., 2020
JPred	Secondary structure prediction server	Free web-based server	Fahmi et al., 2020; Wu, Liu, et al., 2020; Wu, Zhao, et al., 2020
PyMOI	Molecular visualization software	Open source	Ibrahim et al., 2020; Talluri, ; Kirchdoerfer
Rasmol	Molecular visualization software	Open source	Talluri, 2020
Enrichr	Performs gene set enrichment analysis	Free web-based server	Zhou et al., 2020
TMHMM	Transmembrane helices prediction server	Free web-based server	Chan et al., 2020; Wu, Liu, et al., 2020; Wu, Zhao, et al., 2020
ProtScale	Compute profile created by amino acid scale on a specific protein	Free web-based server	Ibrahim et al., 2020
PRODIGY	Predicts binding affinity	Free web-based server	Ibrahim et al., 2020
ViPR	Sequence alignment and analysis server	Free web-based server	Grifoni et al., 2020; Cleemput et al., 2020
Rosetta	Model refinement software	Academic	Kirchdoerfer et al., 2016
Coot	Model building and refinement	Open source	Kirchdoerfer et al., 2016
Genome detective coronavirus typing tool	Assemble all viral genome from NGS datasets	Free web-based server	Cleemput et al., 2020
GLIDE	High-throughput virtual screening software	Open source	Jin et al., 2020

glycoproteins of 2019-nCoV at the C-terminal domain (2019-nCoV-CTD). An experimentally solved structure of hACE2 in complex with 2019-nCoV-CTD suggested similar binding that was observed

between hACE2 and SARS-CoV. Although, stronger binding with a higher affinity toward receptor was observed at the atomic and molecular level due to 2019-nCoV-CTD mutations. Further, a group

of murine monoclonal and polyclonal antibodies that interacted with the SARS-CoV spike protein did not interact with that of 2019-nCoV, implying distinct peculiarity of antigenicity in 2019-nCoV. Such distinctions provide profound insight for being responsible for the life-threatening nature of 2019-nCoV and therefore, must be targeted to develop a therapeutic solution thereby inhibiting the pathogen (Wang et al., 2020). Spike glycoprotein interacting with human glucose-related protein, GRP78 was demonstrated and four distinct regions of the spike glycoprotein were identified to be highly involved in an interaction with the candidate receptor as depicted in Figure 9b (Ibrahim et al., 2020). Host cell surface binding takes place through the S1 subunit followed by viral fusion. Two domains of S1 subunit of various coronaviruses accept different host receptors. S1-CTDs recognize DPP4, APN, and ACE2 protein receptors. S1-CTD, in turn, consists of two subdomains: a core domain and a receptor-binding motif (RBM). RBM has a concave surface to mediate binding to ACE2. RBMs in HCoV-NL63, PRCV, and SARS-CoV may have diverged into ACE1-binding RBDs. The spike protein is present in two different conformations, that is, prefusion and postfusion which undergo transition for membrane fusion. The prefusion structure was determined which was found similar to the influenza virus hemagglutinin. This provided information about the evolution of coronavirus S1. Betacoronavirus S1-NTDs consist of galectin folds which indicate coronavirus S1-NTDs as host origin. Hence, the evolutionary relationship between S1-CTD and host galectins is possible (Li, 2016).

The 2019-nCoV Docking Server was established to determine the binding affinity between the targets and small molecules, peptides, or antibodies using AutoDockVina and CoDockPP software for docking analysis. The server also helps to visualize the docked complexes and hence, an effective tool for 2019-nCoV drug discovery (Kong et al., 2020). Jin et al., 2020 claimed that a combination of structure-based drug design and high-throughput virtual screening can be effective in discovering new drugs to treat 2019-nCoV. Candidate drugs were found to bind at the binding site of the target protein Mpro. N3 inhibitor bound to the target protein Mpro at its binding cavity is depicted in Figure 9c. The binding pockets were observed to be situated between domains I and II (Figure 9d), which seemed to be highly conserved. Figure 9e depicts the key residues of Mpro involved in the interaction with N3 inhibitor and Figure 9f highlights the C-S covalent bond among other interactions. Therefore, binding pockets located between the domains I and II show good binding with antiviral inhibitors (Jin et al., 2020).

Wu et al. (Wu, Liu, et al., 2020; Wu, Zhao, et al., 2020) reported that 21 target proteins of 2019-nCoV, human, and human ACE2 had undergone virtual ligand screening. An accurate evaluation of the docking result was done using ICM-Pro software. Potential compounds were screened from the ZINC database and a natural products database. Compounds such as antiviral drugs, antibacterial drugs, antiasthmatic drugs, and hepatoprotective drugs were identified from the drug library. The natural products, such as flavonoids and xanthenes that interact with 2019-nCoV targets were also identified. Therefore, herbal medicines with these compounds as a majority can be used to treat coronavirus infections. Many compounds were found

to bind to ACE2 but ACE2-Spike complex implied the inhibition of ACE2 rather than viral infection. Natural hesperidin was the only compound found to bind to the receptor-binding domain of the Spike glycoprotein to human ACE2. It was observed from the docking results that spike, RNA dependent RNA polymerase (RdRp), 3C-Like protease, papain-like protease, and several nonstructural proteins are likely to be remedial targets of antivirus drugs. Docking results of Remdesivir-TP and RdRp showed a good binding score of -112.8 indicating to be a potential candidate drug for the treatment of 2019-nCoV pneumonia. Chloroquine phosphate also showed activity against 2019-nCoV; however, it requires further validation. Anti-AIDS drugs, ritonavir, and lopinavir did not bind to the identified targets, thus, they cannot be used for the treatment of coronavirus infections. Future work will focus on the further validation of the activities of screened drugs, drug design, and in vivo and in vitro tests (Wu, Liu, et al., 2020; Wu, Zhao, et al., 2020). To evaluate receptor and receptor-ligand interaction, simulation mechanisms must be emphasized (Robson, 2020). Molecular dynamics (MD) simulations conducted by Zhou et al. suggested changing the intermolecular dynamics in protein-substrate complexes eliminates the mechanism underlying the protease activity. The discovery of novel crucial residues for enzyme activity in the binding pocket could potentially provide more druggable sites for the design of protease inhibitors (Zhou et al., 2019). Recently, it is reported that hydroxychloroquine (HCQ) can efficiently inhibit SARS-CoV-2 infection in vitro (Liu et al., 2020). HCQ is safe and less toxic compared with chloroquine; however, an overdose of HCQ can cause poisoning and death.

In conclusion, the process of understanding the underlying mechanism of 2019-nCoV protein targets interacting with receptor and drug candidates at the molecular level is easier due to computational approaches. Table 2 shows the various computational methods/techniques used. Also, virtually screening various conventional drugs based on effective inhibition can be immediately effective against 2019-nCoV as they are already FDA approved, and virtual screening of novel natural lead compounds against 2019-nCoV protein targets based on pharmacokinetic properties contributes in developing a profound insight for further validation by MD simulation studies, experimental validation involving in vitro and in vivo assays to confirm the predicted results.

6 | CONCLUSION

EM and AFM were used to track the progress of SARS-CoV in the Vero E6 cell surface. They have been used to visualize the changes in the surface topography of SARS-CoV infected cells at late infection stages. The presence of crown-like surface structures in coronavirus were observed in 3D under AFM. These observations help in understanding the interaction of SARS-CoV with the host cells and the progression of the infection. Replication studies were performed with TEM, elucidating thorough intracellular changes in two dimensions. Also, cryo-EM was used to determine the 3D structure of the HCoV-NL63 spike protein and its cellular receptor during infection.

Coronavirus infections can be lethal for cells and the outcome of the infection depends on virus' strains and cell types. Again, fluorescence microscopy provides information to understand how SARS-CoV infects and enters the live host cells which are not possible using an EM. However, the spatial resolution in the fluorescence microscope is limited to the objective lens and excitation wavelength used. In this regard, correlative light electron microscopy (CLEM) can be used in virus studies, which combines the benefits of fluorescence microscopy and electron microscopy to overcome the drawbacks with the individual techniques (Romero-Brey, 2018; Santarella-Mellwig et al., 2018). Along with these techniques, computational biology contributes to understanding the viral mechanism at the molecular and atomic levels paving a path for an alternative therapeutic strategy. Therefore, careful design and clinical trials are required to achieve efficient control of 2019-nCoV.

ACKNOWLEDGMENTS

We thank SERB-Department of Science and Technology (DST), Government of India for the financial support (Project Number—ECR/2016/001944). We thank Dr. K Satyamoorthy, Director, Manipal School of Life Sciences (MSLS), Manipal Academy of Higher Education (MAHE), Manipal, India and Dr. KK Mahato, HoD, Department of Biophysics, MSLS, MAHE, Manipal, India for their constant support and guidance. We would also express our sincere gratitude to MAHE, Manipal for providing the infrastructure needed for the study.

CONFLICT OF INTEREST

The authors declare no conflicts of interest.

ORCID

Sindhoora Kaniyala Melanthota  <https://orcid.org/0000-0002-1546-8226>

Soumyabrata Banik  <https://orcid.org/0000-0002-2254-1428>

Nirmal Mazumder  <https://orcid.org/0000-0001-8068-6484>

REFERENCES

- Akhtar, K., Khan, S. A., Khan, S. B., & Asiri, A. M. (2018). Scanning electron microscopy: Principle and applications in nanomaterials characterization. In *Handbook of materials characterization* (pp. 113–145). Cham: Springer.
- Baker, M. (2018). Cryo-electron microscopy shapes up. *Nature*, *561*(7723), 565–568.
- Beilstein, F., Cohen, G. H., Eisenberg, R. J., Nicolas, V., Esclatine, A., & Padeloup, D. (2019). Dynamic organization of herpesvirus glycoproteins on the viral envelope revealed by super-resolution microscopy. *PLoS Pathogens*, *15*(12), e1008209. <https://doi.org/10.1371/journal.ppat.1008209>
- Cawte, A. D., Unrau, P. J., & Rueda, D. S. (2020). Live cell imaging of single RNA molecules with fluorogenic Mango II arrays. *Nature Communications*, *12*(83), 1–11. <https://doi.org/10.1038/s41467-020-14932-7>
- CDC. 2020. Retrieved from <https://www.cdc.gov/coronavirus/2019-ncov/about/testing.html>
- Ceraolo, C., & Giorgi, F. M. (2020). Genomic variance of the 2019-nCoV coronavirus. *Journal of Medical Virology*, *92*, 522–528. <https://doi.org/10.1002/jmv.25700>
- Chan, F. W. J., Kok, H. K., Zhu, Z., Chu, H., Wang To, K. K., Yuan, S., & Yuen, Y. K. (2020). Genomic characterization of the 2019 novel human pathogenic coronavirus isolated from a patient with atypical pneumonia after visiting Wuhan. *Emerging Microbes & Infections*, *9*(1), 221–236. <https://doi.org/10.1080/22221751.2020.1719902>
- Chang, L., Yan, Y., & Wang, L. (2020). Coronavirus disease 2019: Coronaviruses and blood safety. *Transfusion Medicine Reviews*, *34*, 75–80. <https://doi.org/10.1016/j.tmr.2020.02.003>
- Ciejka, J., Wolski, K., Nowakowska, M., Pyrc, K., & Szczubiatka, K. (2017). Biopolymeric nano/microspheres for selective and reversible adsorption of coronaviruses. *Materials Science and Engineering: C*, *76*, 735–742. <https://doi.org/10.1016/j.msec.2017.03.047>
- Cleemput, S., Dumon, W., Fonseca, V., Karim, W. A., Giovanetti, M., Alcantara, L. C., & De Oliveira, T. (2020). Genome detective coronavirus typing tool for rapid identification and characterization of novel coronavirus genomes. *BioRxiv*, *36*, 3552–3555. <https://doi.org/10.1093/bioinformatics/btaa145>
- Däder, B., Burckbuchler, M., Macia, J. L., Alcon, C., Curie, C., Gargani, D., ... Drucker, M. (2019). Split green fluorescent protein as a tool to study infection with a plant pathogen, cauliflower mosaic virus. *PLoS One*, *14*(3), e0213087. <https://doi.org/10.1371/journal.pone.0213087>
- Diaspro, A. (Ed.). (2010). *Optical fluorescence microscopy: From the spectral to the nano dimension*. London: Springer Science & Business Media.
- Drygin, Y. F., Bordunova, O. A., Gallyamov, M. O., & Yaminsky, I. V. (1998). Atomic force microscopy examination of tobacco mosaic virus and virion RNA. *FEBS Letters*, *425*(2), 217–221. [https://doi.org/10.1016/s0014-5793\(98\)00232-4](https://doi.org/10.1016/s0014-5793(98)00232-4)
- Eaton, P., & West, P. (2010). *Atomic force microscopy*. Oxford: Oxford University Press.
- Epand, R. F., Yip, C. M., Chernomordik, L. V., LeDuc, D. L., Shin, Y. K., & Epand, R. M. (2001). Self-assembly of influenza hemagglutinin: Studies of ectodomain aggregation by in situ atomic force microscopy. *Biochimica et Biophysica Acta (BBA)-Biomembranes*, *1513*(2), 167–175. [https://doi.org/10.1016/S0005-2736\(01\)00350-9](https://doi.org/10.1016/S0005-2736(01)00350-9)
- Fahmi, M., Kubota, Y., & Ito, M. (2020). Nonstructural proteins NS7b and NS8 are likely to be phylogenetically associated with evolution of 2019-nCoV. *Infections, Genetics & Evolution*, *81*, 104272. <https://doi.org/10.1016/j.meegid.2020.104272>
- Goldsmith, C. S., & Miller, S. E. (2009). Modern uses of electron microscopy for detection of viruses. *Clinical Microbiology Reviews*, *22*(4), 552–563. <https://doi.org/10.1128/CMR.00027-09>
- Goldsmith, C. S., Tatti, K. M., Ksiazek, T. G., Rollin, P. E., Comer, J. A., Lee, W. W., & Zaki, S. R. (2004). Ultrastructural characterization of SARS coronavirus. *Emerging Infectious Diseases*, *10*(2), 320–326. <https://doi.org/10.3201/eid1002.030913>
- Grifoni, A., Sidney, J., Zhang, Y., Scheuermann, R. H., Peters, B., & Sette, A. (2020). A sequence homology and Bioinformatic approach can predict candidate targets for immune responses to SARS-CoV-2. *Cell Host and Microbe*, *27*(4), 671–680. <https://doi.org/10.1016/j.chom.2020.03.002>
- Guarner, J. (2020). Three emerging coronaviruses in two decades: The story of SARS, MERS, and now COVID-19. *American Journal of Clinical Pathology*, *153*(4), 420–421. <https://doi.org/10.1093/ajcp/aqaa029>
- Ibrahim, I. M., Abdelmalek, D. H., Elshahat, M. E., & Elfiky, A. A. (2020). COVID-19 spike-host cell receptor GRP78 binding site prediction. *The Journal of Infection*, *S0163-4453*(20), 30107. <https://doi.org/10.1016/j.jinf.2020.02.026>
- Jin, Z., Du, X., Xu, Y., Deng, Y., Liu, M., Zhao, Y., ... Duan, Y. (2020). Structure of M pro from SARS-CoV-2 and discovery of its inhibitors. *Nature*, *582*, 289–293. <https://doi.org/10.1101/2020.02.26.964882>
- Kim, M., Cho, M., Lee, J. H., Kim, H., & Son, H. S. (2019). Analysis of coronavirus spike proteins and virus–host interactions. *The Korean Journal of Public Health*, *56*(1), 25–32. <https://doi.org/10.17262/KJPH.2019.06.56.1.25>

- Kirchdoerfer, R. N., Cottrell, C. A., Wang, N., Pallesen, J., Yassine, H. M., Turner, H. L., ... Ward, A. B. (2016). Pre-fusion structure of a human coronavirus spike protein. *Nature*, 531(7592), 118–121. <https://doi.org/10.1038/nature17200>
- Knoops, K., Kikkert, M., van den Worm, S. H., Zevenhoven-Dobbe, J. C., van der Meer, Y., Koster, A. J., ... Snijder, E. J. (2008). SARS-coronavirus replication is supported by a reticulovesicular network of modified endoplasmic reticulum. *PLoS Biology*, 6(9), e226. <https://doi.org/10.1371/journal.pbio.0060226>
- Kong, R., Yang, G., Xue, R., Liu, M., Wang, F., Hu, J., ... Chang, S. (2020). COVID-19 docking server: An interactive server for docking small molecules, peptides and antibodies against potential targets of COVID-19. *arXiv* 2003.00163v1.
- Ksiazek, T. G., Erdman, D., Goldsmith, C. S., Zaki, S. R., Peret, T., Emery, S., ... Rollin, P. E. (2003). A novel coronavirus associated with severe acute respiratory syndrome. *New England Journal of Medicine*, 348(20), 1953–1966. <https://doi.org/10.1056/NEJMoa030781>
- Kumar, A., Kim, J. H., Ranjan, P., Metcalfe, M. G., Cao, W., Mishina, M., ... York, I. (2017). Influenza virus exploits tunneling nanotubes for cell-to-cell spread. *Scientific Reports*, 7(1), 1–14. <https://doi.org/10.1038/srep40360>
- Kuznetsov, Y. G., & McPherson, A. (2011). Atomic force microscopy in imaging of viruses and virus-infected cells. *Microbiology and Molecular Biology Reviews: MMBR*, 75(2), 268–285. <https://doi.org/10.1128/MMBR.00041-10>
- Lee, C. K., Lin, C. W., Lin, S., Lee, A. S. Y., Wu, J. Y., Lee, S. S., ... Wang, A. B. (2004). From an integrated biochip detection system to a defensive weapon against the SARS-CoV virus: OBMorph. *MRS Online Proceedings Library Archive*, 820. <https://doi.org/10.1557/PROC-820-O9.8>
- Li, F. (2016). Structure, function, and evolution of coronavirus spike proteins. *Annual Review of Virology*, 3, 237–261. <https://doi.org/10.1146/annurev-virology-110615-042301>
- Lichtman, J. W., & Conchello, J. A. (2005). Fluorescence microscopy. *Nature Methods*, 2(12), 910–919. <https://doi.org/10.1038/nmeth1205-902>
- Lin, S., Lee, C. K., Lee, S. Y., Kao, C. L., Lin, C. W., Wang, A. B., ... Huang, L. S. (2005). Surface ultrastructure of SARS coronavirus revealed by atomic force microscopy. *Cellular Microbiology*, 7(12), 1763–1770. <https://doi.org/10.1111/j.1462-5822.2005.00593.x>
- Lin, Y., Yan, X., Cao, W., Wang, C., Feng, J., Duan, J., & Xie, S. (2004). Probing the structure of the SARS coronavirus using scanning electron microscopy. *Antiviral Therapy*, 9, 287–289.
- Liu, D. X., & Inglis, S. C. (1991). Association of the infectious bronchitis virus 3c protein with the virion envelope. *Virology*, 185(1991), 911–917. [https://doi.org/10.1016/0042-6822\(91\)90572-s](https://doi.org/10.1016/0042-6822(91)90572-s)
- Liu, J., Cao, R., Xu, M., Wang, X., Zhang, H., Hu, H., & Wang, M. (2020). Remdesivir and chloroquine effectively inhibit the recently emerged novel coronavirus (2019-nCoV) in vitro. *Cell Research-Nature*, 30, 269–271. <https://doi.org/10.1038/s41421-020-0156-0>
- Lu, Y., Liu, D. X., & Tam, J. P. (2008). Lipid rafts are involved in SARS-CoV entry into Vero E6 cells. *Biochemical and Biophysical Research Communications*, 369(2), 344–349. <https://doi.org/10.1016/j.bbrc.2008.02.023>
- Manopo, I., Lu, L., He, Q., Chee, L. L., Chan, S. W., & Kwang, J. (2005). Evaluation of a safe and sensitive spike protein-based immunofluorescence assay for the detection of antibody responses to SARS-CoV. *Journal of Immunological Methods*, 296(1–2), 37–44. <https://doi.org/10.1016/j.jim.2004.10.012>
- Masters, P. S. (2006). The molecular biology of coronaviruses. *Advances in Virus Research*, 66, 193–292. [https://doi.org/10.1016/S0065-3527\(06\)66005-3](https://doi.org/10.1016/S0065-3527(06)66005-3)
- Mazumder, N., Lyn, R. K., Singaravelu, R., Ridsdale, A., Moffatt, D. J., Hu, C. W., & Pezacki, J. P. (2013). Fluorescence lifetime imaging of alterations to cellular metabolism by domain 2 of the hepatitis C virus core protein. *PLoS One*, 8(6), e66738. <https://doi.org/10.1371/journal.pone.0066738>
- Monteil, V., Kwon, H., Prado, P., Hagelkrüys, A., Wimmer, R. A., Stahl, M., ... Romero, J. P. (2020). Inhibition of SARS-CoV-2 infections in engineered human tissues using clinical-grade soluble human ACE2. *Cell*, 181(4), 905–913. <https://doi.org/10.1016/j.cell.2020.04.004>
- Ng, M. L., Lee, J. W. M., Leong, M. L. N., Ling, A. E., Tan, H. C., & Ooi, E. E. (2004). Topographic changes in SARS coronavirus-infected cells at late stages of infection. *Emerging Infectious Diseases*, 10(11), 1907–1914. <https://doi.org/10.3201/eid1011.040195>
- Oshiro, L. S., Schieble, J. H., & Lennette, E. H. (1971). Electron microscopic studies of coronavirus. *Journal of General Virology*, 12(2), 161–168. <https://doi.org/10.1099/0022-1317-12-2-161>
- Parot, P., Dufrene, Y. F., Hinterdorfer, P., Le Grimmelc, C., Navajas, D., Pellequer, J.-L., & Scheuring, S. (2007). Past, present and future of atomic force microscopy in life sciences and medicine. *Journal of Molecular Recognition*, 20(6), 418–431. <https://doi.org/10.1002/jmr.857>
- Pillaiyar, T., Meenakshisundaram, S., & Manickam, M. (2020). Recent discovery and development of inhibitors targeting coronaviruses. *Drug Discovery Today*, 25, 668–688. <https://doi.org/10.1016/j.drudis.2020.01.015>
- Plomp, M., Rice, M. K., Wagner, E. K., McPherson, A., & Malkin, A. J. (2002). Rapid visualization at high resolution of pathogens by atomic force microscopy: Structural studies of herpes simplex virus-1. *The American Journal of Pathology*, 160(6), 1959–1966. [https://doi.org/10.1016/S0002-9440\(10\)61145-5](https://doi.org/10.1016/S0002-9440(10)61145-5)
- Prasad, S., Potdar, V., Cherian, S., Abraham, P., & Basu, A. (2020). Transmission electron microscopy imaging of SARS-CoV-2. *Indian Journal of Medical Research*, 151(2–3), 241–243. https://doi.org/10.4103/ijmr.IJMR_577_20
- Robson, B. (2020). Computers and viral diseases. Preliminary bioinformatics studies on the design of a synthetic vaccine and a preventative peptidomimetic antagonist against the SARS-CoV-2 (2019-nCoV, COVID-19) coronavirus. *Computers in Biology and Medicine*, 119, 103670. <https://doi.org/10.1016/j.combiomed.2020.103670>
- Romero-Brey, I. (2018). 3D electron microscopy (EM) and correlative light electron microscopy (CLEM) methods to study virus-host interactions. *Methods in Molecular Biology*, 1836, 213–236.
- Santarella-Mellwig, R., Haselmann, U., Schieber, N. L., Walther, P., Schwab, Y., Antony, C., ... Romero-Brey, I. (2018). Correlative light electron microscopy (CLEM) for tracking and imaging viral protein associated structures in cryo-immobilized cells. *Journal of Visualized Experiments*, (139), e58154. <https://doi.org/10.3791/58154>
- Siddell, S. G., Anderson, R., Cavanagh, D., Fujiwara, K., Klenk, H. D., Macnaughton, M. R., & van der Zeijst, B. A. M. (1983). Coronaviridae. *Intervirology*, 20(4), 181–189. <https://doi.org/10.1159/000149390>
- Sieczkarski, S. B., & Whittaker, G. R. (2002). Dissecting virus entry via endocytosis. *Journal of General Virology*, 83(7), 1535–1545. <https://doi.org/10.1099/0022-1317-83-7-1535>
- Spaan, W., Cavanagh, D., & Horzinek, M. C. (1988). Coronaviruses: Structure and genome expression. *Journal of General Virology*, 69(12), 2939–2952. <https://doi.org/10.1099/0022-1317-69-12-2939>
- Walls, A. C., Tortorici, M. A., Frenz, B., Snijder, J., Li, W., Rey, F. A., & Velesler, D. (2016). Glycan shield and epitope masking of a coronavirus spike protein observed by cryo-electron microscopy. *Nature Structural and Molecular Biology*, 23(10), 899–905. <https://doi.org/10.1038/nsmb.3293>
- Wang, H., Yang, P., Liu, K., Guo, F., Zhang, Y., Zhang, G., & Jiang, C. (2008). SARS coronavirus entry into host cells through a novel clathrin-and caveolae-independent endocytic pathway. *Cell Research*, 18(2), 290–301. <https://doi.org/10.1038/cr.2008.15>
- Wang, Q., Zhang, Y., Wu, L., Niu, S., Song, C., Zhang, Z., ... Qi, J. (2020). Structural and functional basis of SARS-CoV-2 entry by using human ACE2. *Cell*, 181, 894–904. <https://doi.org/10.1016/j.cell.2020.03.045>

- WHO. 2014. Cumulative number of reported probable cases of severe acute respiratory syndrome (SARS). Retrieved from <https://www.who.int/csr/sars/country/en>
- WHO. 2019. MERS Situation update, November 2019. Retrieved from <https://www.who.int/emergencies/mers-cov/en>
- WHO. 2020. Retrieved from https://www.who.int/docs/default-source/coronaviruse/situation-reports/20200320-sitrep-60-covid-19.pdf?sfvrsn=d2bb4f1f_2
- Williams, D. B., & Carter, C. B. (1996). *Transmission electron microscopy*. Boston, MA: Springer.
- Woo, P. C. Y., Lau, S. K. P., Li, K. S. M., Poon, R. W. S., Wong, B. H. L., Tsoi, H., ... Yuen, K. (2006). Molecular diversity of coronaviruses in bats. *Virology*, 351(1), 180–187. <https://doi.org/10.1016/j.virol.2006.02.041>
- Wu, C., Liu, Y., Yang, Y., Zhang, P., Zhong, W., Wang, Y., & Zheng, M. (2020). Analysis of therapeutic targets for SARS-CoV-2 and discovery of potential drugs by computational methods. *Acta Pharmaceutica Sinica B*, 10, 766–788. <https://doi.org/10.1016/j.apsb.2020.02.008>
- Wu, F., Zhao, S., Yu, B., Chen, Y.-M., Wang, W., Song, Z.-G., & Zhang, Y.-Z. (2020). A new coronavirus associated with human respiratory disease in China. *Nature*, 579, 265–269. <https://doi.org/10.1038/s41586-020-2008-3>
- Yang, J. (2004). AFM as a high-resolution imaging tool and a molecular bond force probe. *Cell Biochemistry and Biophysics*, 41(3), 435–450. <https://doi.org/10.1385/CBB:41:3:435>
- Yuan, X., Li, J., Shan, Y., Yang, Z., Zhao, Z., Chen, B., & Cong, Y. (2005). Subcellular localization and membrane association of SARS-CoV 3a protein. *Virus Research*, 109(2), 191–202. <https://doi.org/10.1016/j.virusres.2005.01.001>
- Yuan, X., Wu, J., Shan, Y., Yao, Z., Dong, B., Chen, B., & Cong, Y. (2006). SARS coronavirus 7a protein blocks cell cycle progression at G0/G1 phase via the cyclin D3/pRb pathway. *Virology*, 346(1), 74–85. <https://doi.org/10.1016/j.virol.2005.10.015>
- Zaki, A. M., Van Boheemen, S., Bestebroer, T. M., Osterhaus, A. D., & Fouchier, R. A. (2012). Isolation of a novel coronavirus from a man with pneumonia in Saudi Arabia. *The New England Journal of Medicine*, 367(19), 1814–1820. <https://doi.org/10.1056/NEJMoa1211721>
- Zgheib, S., Lysova, I., Réal, E., Dukhno, O., Vauchelles, R., Pires, M., & Mély, Y. (2019). Quantitative monitoring of the cytoplasmic release of NCp7 proteins from individual HIV-1 viral cores during the early steps of infection. *Scientific Reports*, 9(1), 1–14. <https://doi.org/10.1038/s41598-018-37150-0>
- Zhang, L., Lin, D., Sun, X., Curth, U., Drosten, C., Sauerhering, L., ... Hilgenfeld, R. (2020). Crystal structure of SARS-CoV-2 main protease provides a basis for design of improved α -ketoamide inhibitors. *Science*, 368(6489), 409–412. <https://doi.org/10.1126/science.abb3405>
- Zhou, J., Fang, L., Yang, Z., Xu, S., Lv, M., Sun, Z., ... Xiao, S. (2019). Identification of novel proteolytically inactive mutations in coronavirus 3C-like protease using a combined approach. *The FASEB Journal*, 33, 14575–14587. <https://doi.org/10.1096/fj.201901624RR>
- Zhou, Y., Hou, Y., Shen, J., Huang, Y., Martin, W., & Cheng, F. (2020). Network-based drug repurposing for novel coronavirus 2019-nCoV/SARS-CoV-2. *Cell Discovery*, 6(1), 1–18. <https://doi.org/10.1038/s41421-020-0153-3>

How to cite this article: Kaniyala Melanthota S, Banik S, Chakraborty I, et al. Elucidating the microscopic and computational techniques to study the structure and pathology of SARS-CoVs. *Microsc Res Tech*. 2020;83: 1623–1638. <https://doi.org/10.1002/jemt.23551>